ISSN 1063-7729, Astronomy Reports, 2010, Vol. 54, No. 6, pp. 496–508. © Pleiades Publishing, Ltd., 2010.
Original Russian Text © S.V. Polushkin, I.E. Val'tts, 2010, published in Astronomicheskiĭ Zhurnal, 2010, Vol. 87, No. 6, pp. 546–559.

Class I Methanol Emission Around DR 21(OH)

S. V. Polushkin and I. E. Val'tts

Astro Space Center, Lebedev Physical Institute, Russian Academy of Sciences, Profsoyuznaya ul. 84/32, Moscow 117997, Russia

Received November 20, 2009; in final form, November 26, 2009

Abstract—Results of new observations of the vicinity of DR 21(OH) conducted on the 20-m Onsala radio telescope are presented. The goal was to search for associations between molecular hydrogen emission tracing shock waves and class I methanol maser emission. Observations at 44 and 36 GHz have shown that an extensive region of faint methanol maser emission elongated North–South is probably present in the vicinity of DR 21(OH). The linear size of this structure may be a factor of ten larger than the central region in DR 21(OH) that emits at 44 GHz. Three maser emission peaks are clearly visible in the northern (DR 21N), central (DR 21(OH)), and southern (vicinity of DR 21West) parts of this structure. Many other structures are also embedded in this region, including the protostellar disk ERO 3 previously detected at 6.7 GHz. Maser components of these objects are formed with velocities from −5 to −2 km/s, with a velocity gradient from −5 in the North to −2 km/s in the South. The spatial resolution of the map is not high enough to distinguish fine structures at 44 GHz associated with spots and jets emitting in molecular hydrogen.

DOI: 10.1134/S106377291006003X

1. INTRODUCTION

According to modern concepts, class I methanol maser emission is a typical sign of the presence of active star-forming processes in the interstellar medium. The mechanism exciting these masers (at frequencies of 25, 36, and 84 GHz in *E*-methanol and 44, 95, and 146 GHz in *A*-methanol) is being actively researched. A number of studies have analyzed the possible effects of radiation on the population densities of corresponding levels (see, e.g., [1]). However, the view that the dominating pumping mechanism for such masers is collisional is more widespread [2, 3]; i.e., the excitation and deactivation of the molecular levels are realized inside a maser condensation, without the need for external radiation.

Collisional pumping is sensitive to density variations in the maser condensation. The density can change under the action of a shock front flowing around the condensation; such masers can be produced, e.g., by a bipolar outflow [4, 5]. At the same time, statistical analyses of all presently known class I methanol masers has shown that only a quarter are associated with bipolar outflows [6].

Bipolar outflows are observed in several CO lines toward DR 21(OH), in various transitions and isotopes that strongly differ in their position angles and the wing span of the lines [7–10]. However, there is no concensus that any of these outflows is responsible for the excitation of methanol masers, since they do not correspond to large-scale structures that are close in velocity and orientation to the distribution of methanol maser components observed at 95 GHz [11] and 44 GHz [12].

At the same time, note that none of the outflows detected in CO has been confirmed by observations in the H_2 1-0 S(1) line at 2.12 μm [13, 14], which is also a tracer of moving gas: molecular hydrogen is excited in a medium that was exposed to the effect of a shock front. The presence of emission in this line implies the existence of a bipolar outflow front or another active dynamic process in the medium around the condensation (see, e.g., [15] and references therein). According to [13, 14], only weakly emitting clumpy structure is visible in the molecular hydrogen lines around DR 21(OH) (probably, due to strong extinction), which does not look like a single entity in the form of a bipolar outflow of the sort observed, e.g., in DR 21.

The dense gas in DR 21(OH) represents a structure elongated from Northeast to Southwest and oriented along a line connecting two millimeter continuum sources, MM1 and MM2, observed in the central part of this region [7, 16]. The configuration of the material emitting thermal methanol lines [5] differs from that observed in thermal lines of NH_3, CS, or $C^{18}O$, though it demonstrates, like the NH_3, a hotter and denser gas around the brighter and more compact source of millimeter emission MM1. As was shown in [5], no association between the thermal methanol emission and components of methanol maser emission has been observed; it is not possible to trace

the presence of moving material from the profiles of thermal methanol lines.

Many authors [13, 16–18] consider the configuration of methanol maser spots in DR 21(OH), almost orthogonal to the MM1–MM2 axis, observed at 95 and 44 GHz, to be bipolar, and the two clusters of maser features concentrated at different radial velocities (at approximately 0 and −5 km/s) to be outflow lobes.

The methanol maser has a distant component [17]. This component does not belong to the region in which OH and H_2O masers are concentrated and does not coincide with the overall methanol maser structure, which is in the form of two clusters of spatially separated maser condensations. We have confirmed the existence of this component using archival VLA data for 2003 for the 44-GHz maser [19, Fig. 5]. It is projected against a bright H_2 filament on the infrared map of Davis et al. [13], and is located to the north from the main methanol maser chain. Precisely this fact has motivated us to study other filaments of approximately the same, fairly weak intensity, since it is known that, e.g., the H_2-bright region DR 21 is not a zone of methanol emission activity, probably because the shock should be slow that its passage does not fully destruct the grain mantles supplying free methanol to the interstellar medium, in other words, does not dissociate the methanol [20].

To find out whether this coincidence with an H_2 filament is accidental or there is some association between the methanol and molecular hydrogen emission, and also to search for new maser components, we have observed individual knots at 36 and 44 GHz and mapped the DR 21(OH) neighborhood at 44 GHz outside the structure of the main class I methanol maser aggregate, in directions free of HII regions. A similar study was carried out by Pratap et al. [21]. We compare the results of Pratap et al. and our work in the Discussion.

2. OBSERVATIONS AND RESULTS

The observations were conducted on the 20-m radio telescope in Onsala (Sweden) in two stages. The first observing session was carried out from November 29 to December 5, 2007, at 36169.2400 MHz in the $4_{-1}-3_0E$ transition and at 44069.4900 MHz in the $7_0-6_1A^+$ transition toward the maser DR 21(OH) and six positions of map "B" of Davis et al. [13], including the bright spot, jets, and arcs of H_2 emission. We also studied the extremely reddened object ERO 3, in which a class II methanol maser was recently detected [22, 23]. The beamwidth was 105″ at 36 GHz and 88″ at 44 GHz.

The aperture efficiency was 53%; in both cases, this corresponds to approximately 18 Jy/K of corrected antenna temperature. The spectrometer used was a 1600-channel autocorrelator with a bandwidth of 20 MHz. Some spectra were taken at 44 GHz with a frequency resolution of 12.5 kHz, or radial velocity resolution 0.09 km/s, and others with a resolution of 25 kHz, or 0.17 km/s. At 36 GHz, all the spectra were recorded with a resolution of 25 kHz, or 0.21 km/s. The calibration was done using the standard chopper-wheel method [24]. The system noise temperature during the observations was 150 K or more, depending on the source elevation and weather conditions. The observations were conducted in the ON–ON mode by beam switching; the beam separation was 11′ in the azimuth.

The results of the first stage of the observations are listed in Table 1 (44 GHz) and in Table 2 (36 GHz). The pointing positions are given in Table 3. The columns of Tables 1 and 2 list (1) the name of the position in the notation of Davis et al. [13], (2) the ordinal numbers of spectral line components, (3), (4) the line-of-sight velocity and spectral width, (5) peak flux density, and (6) the integrated flux. The line parameters were determined from Gaussian fitting using the XS software of P. Bergman (http://www.chalmers.se/rss/oso-en/observations/data-reduction-software). The spectra are presented in Figs. 1–3, and commentary is given in the Discussion.

We detected methanol emission in five of six 2-μm emission knots studied, as well as toward ERO 3. However, because the beam is larger than 1′, we could not determine the point to which the emission peak refers.

Therefore, from December 5 to 11, 2008, we obtained further observations in order to refine the coordinates and extent of the detected sources. We mapped the region centered at coordinates of DR 21(OH) RA = $20^h39^m01.01^s$, DEC = 42°22′50.2″ (J2000) in the $7_0-6_1A^+$ 44-GHz methanol maser line in 15 40″ cells in right ascension and 11 cells in declination; i.e., within an area (600″ × 400″) in size. Figure 4 shows the grid for these observations. The receiver parameters were the same as in 2007, but the spectral resolution was 25 kHz, or 0.17 km/s. Figures 5 and 6 present the results of mapping the vicinity of the maser DR 21(OH) at 44 GHz, including seven individual positions studied with our first set of observations; these will be considered below.

3. DISCUSSION

In the neighborhood of DR 21(OH), there is a multitude of bright sources emitting at various wavelengths. We list some in Table 3; these are the main sources in the immediate vicinity of DR 21(OH),

Table 1. Parameters of 44 GHz maser lines in the vicinity of DR 21(OH) toward bright spots, jets, and H_2 arcs, from North to South (notation from Davis et al. [13]; pointing positions are listed in Table 3)

Pointing direction	Line component	V_{LSR}, km/s	ΔV, km/s	Flux density, Jy	Integrated flux, Jy km/s
B 9-1 h	1	−4.7	0.5	34.2	19.6
	2	−3.9	0.5	11.0	6.0
	3	−3.5	0.3	7.0	2.6
	4	−2.5	0.5	14.6	7.9
DR 21N*	1	−4.6	0.3	35.2	10.5
	2	−3.6	0.2	2.0	0.5
		−2.6	0.4	7.3	2.4
B 12-1 : B 12-2		–	–	<6	–
ERO 3	1	0.4	0.4	14.6	6.2
	2	0.9	0.3	15.9	5.1
B 6-3	1	0.1	0.9	8.7	8.3
	2	1.2	0.3	10.3	2.2
B 6-1	1	0.4	0.6	147.0	93.4
	2	0.9	0.4	101.0	42.8
DR 21(OH)	1	0.4	0.6	212.2	135.0
	2	0.9	0.4	150.4	63.7
B 4-1	1	−4.0	0.7	7.1	5.2
	2	−2.0	0.7	11.1	8.2
	3	0.6	0.9	8.1	7.7
B 3-1		–	–	<1.6	–
B 1-1 : B 1-3	1	−2.0	0.8	16.1	13.6
DR 21West	1	−2.1	0.5	174.0	92.2

*Line parameters in DR 21N were obtained with the map from the spectrum of Fig. 2.

molecular hydrogen emission knots we study here, and several sources with a common designation "N" ("northern"), which is somewhat confusing. Before proceeding to a discussion of our results, we will analyze this situation in more detail.

Large-scale studies have shown that the densest gas emitting in $C^{18}O$, NH_3, and $C^{34}S$ molecular lines has radial velocities from 0 to −5 km/s and extends to the North, from the older DR 21 region, with a well developed HII region, to the younger DR 21(OH) region (i.e., W75S), in which there is no HII region, but there are infrared and maser sources (see, e.g., [27] and references therein).

The observations of Mangum et al. [7] carried out on the millimeter-wave interferometer of the Owens Valley Radio Observatory (USA) with a resolution of 7″ at 2.7 mm in the continuum and in the $J = 1\text{-}0$ $C^{18}O$ line around DR 21(OH) have shown that the molecular cloud contains at least three compact regions in a $1.0' \times 1.5'$ area (with a linear size of approximately 45 000 AU); in the brightest of these, DR 21(OH)main, two sources (MM1 and MM2) separated by a projected distance of 8″ were earlier detected at 1.4 mm [28]. These are warm, massive cores with associated OH and H_2O masers. According to [7], they are young prestellar objects deeply embedded in the gas–dust material. In turn,

Table 2. Parameters of 36 GHz maser lines in the vicinity of DR 21(OH) toward bright spots, jets, and H_2 arcs, from North to South (notation from Davis et al. [13]; pointing positions are listed in Table 3)

Pointing direction	Line component	V_{LSR}, km/s	ΔV, km/s	Flux density, Jy	Integrated flux, Jy km/s
B 9-1 h	1	−5.5	1.2	4.5	5.7
	2	−4.3	0.8	3.9	3.3
	3	−3.1	1.2	6.3	8.0
	4	0.4	1.2	13.4	17.0
B 12-1 : B 12-2		–	–	<3	–
ERO 3	1	−5.3	0.6	4.8	3.1
	2	−3.5	1.7	7.0	12.6
	3	−1.6	0.5	3.6	1.9
B 6-1	1	−4.7	1.4	7.1	10.5
	2	−3.5	1.1	4.5	5.2
	3	−2.9	0.3	2.5	0.8
	4	−1.9	3.3	6.4	22.4
	5	0.1	0.8	8.4	7.1
B 4-1	1	−4.2	0.9	8.5	8.1
	2	−3.3	0.6	8.9	5.7
B 3-1	1	−4.3	0.4	4.6	1.9
	2	−3.5	1.0	4.4	4.7
	3	−2.6	0.3	1.8	0.6
B 1-1 : B 1-3	1	−2.8	0.7	9.5	7.0
DR 21West	1	−2.7	0.6	23.2	14.7
	2	−1.6	1.2	5.6	7.1
	3	−0.5	0.3	4.1	1.3

the source MM1 has a northeast component, a 20 μm infrared continuum source that does not emit in either molecular lines or in the millimeter. This is a dust-enshrouded young star. Another two warm ($T_K \geq$ 20 K) but less dense continuum sources are visible at 2.7 mm, DR 21(OH)W and DR 21(OH)S, which have no associated OH or H_2O masers; these are early B stars. As a whole, the region is intermediate in its size and luminosity between the ρ Oph molecular core and the Ori KL nebula. We have plotted the millimeter continuum sources MM1 and MM2 on our map (Fig. 5) as open triangles.

VLA observations of the same authors with a higher spatial resolution (4″) at 23 GHz in the thermal (1,1) and (2,2) NH_3 lines, which trace dense gas, added another source, DR 21(OH)N (i.e., labeled "N", northern), which consists of several dense clumps [16, Fig. 3a] and is located approximately 1′ to the North of DR 21(OH)main (hash sign in Fig. 5). This source was detected earlier in the far infrared at 800 and 1100 μm via the emission of surrounding dust [29].

One more source is also labeled "northern" in the following paper. In their study of regions of formation of massive stars, Harvey-Smith et al. [22] searched for class II methanol emission toward DR 21(OH) and DR 21(OH)N. They gave the source ERO 3, which does not coincide with DR 21(OH)N of Mangum et al. [16] and is located approximately 2′ to the North of DR 21(OH)main, an "N" (northern)

Table 3. Some bright sources in the DR 21(OH) neighborhood at various wavelengths, from North to South

No.	Name	α (J2000)	δ (J2000)	$\Delta\alpha$	$\Delta\alpha$	$\Delta\delta$	Comments and references
1	B 9-1 h	$20^h39^m04.6^s$	42°26′07.8″	3.05^s	45.75″	197.6″	Series of bright H_2 spots [13]. Emission at 36 and 44 GHz (this paper)
2	DR 21N	20 39 02.00	42 25 43.0	0.99	14.85	172.8	Emission at 36 and 44 GHz [21] and this paper
3	DR 21(OH)N	20 39 00.38	42 24 38.4	−0.63	−9.45	107.0	Class II maser at 6.7 GHz [22, 23]
4	DR 21(OH)N	20 39 00.46	42 24 36.6	−0.54	−8.10	106.4	ERO 3, bright source at 8 μm [13]
5	B 12-1 : B 12-2	20 38 45.9	42 24 16	−15.61	−234.15	127.8	Bright H_2 spots within a faint diffuse jet [13]
6	DR 21(OH)N	20 38 59.80	42 23 32.7	−1.21	−18.15	42.5	NH_3(1,1), dense core [16]
7	B 6-1 : B 6-3	20 39 00.2	42 23 02				Bright jet [13]
8	DR 21(OH)	20 39 01.01	42 22 50.2	0.0	0.0	0.0	Pointlike source at 8 μm [25], class II maser at 6.7 GHz 1′ to the east in RA [22, 23, 26]
9	MM1	20 39 01.02	42 22 49.8	0.01	0.15	−0.4	Continuum emission peak at 2.7 mm [7]
10	DR 21(OH)	20 38 59.16	42 22 48.9	1.85	−27.75	−1.3	Extreme northwest component of a class I methanol maser, 44 GHz [19]
11	MM2	20 39 00.42	42 22 46.8	−0.59	−8.85	−3.4	Continuum emission peak at 2.7 mm [7]
12	DR 21(OH)	20 39 02.21	42 22 43.9	1.20	18.0	−6.3	Extreme southeast component of a class I methanol maser, 44 GHz [19]
13	B 4-1	20 38 58.3	42 21 09	−2.71	−40.65	−101.2	Prolate arc [13]
14	B 3-1 : B 3-2	20 38 59.9	42 20 51				Trace of H_2 emission [13]
15	B 1-1 : B 1-3	20 38 53.1	42 20 08	−7.91	−118.65	−162.2	Jet and arc [13]
16	DR 21West	20 38 54.78	42 19 21.8	−6.23	−93.45	208.4	Maser at 36 and 44 GHz [5]

designation. Their observations were conducted at 6.7 GHz on MERLIN (Multi-Element Radio-Linked Interferometer Network, Great Britain). Their goal was to search for bipolar outflows and interstellar disks accompanying star formation. Two peaks of strong emission were detected toward DR 21(OH)N/ERO 3, and weaker emission toward DR 21(OH).

Finally, Pratap et al. [21] recently reported the results of observations similar to those we consider here. This paper was published in 2008, but the observations were carried out earlier, from 2000 to 2005, and their aims were somewhat broader. As we do in [6], Pratap et al. [21] note that class I methanol emission has always been searched for only in known star-forming regions and never using an independent sample. They attempted to increase the number of class I methanol masers studied at 44 GHz in the vicinity of already known maser sources, targeting the same known star-forming regions, in particular, DR 21(OH). When they detected a new 44-GHz maser, it was also studied at the other class I frequencies of 25, 36, and 95 GHz. The observations at 44 and 36 GHz were carried out with the 37-m Haystack Observatory radio telescope with a beamwidth of 46″ at 44 GHz. Results were presented for 320″ × 560″ areas with a cell size similar to our Onsala observations (40″), as well as for some additional pointings for 120″ × 120″ areas with a cell size of 20″. The spectral resolution in the Haystack observations was 2 kHz, approximately a factor of six higher than for the Onsala observations. Emission at 44 and 36 GHz was detected toward three known sources, DR 21-W, DR 21-C, and DR 21(OH), as well as one new source, labeled DR 21N [21]. This new maser lies to the North of the dense condensation DR 21(OH)N

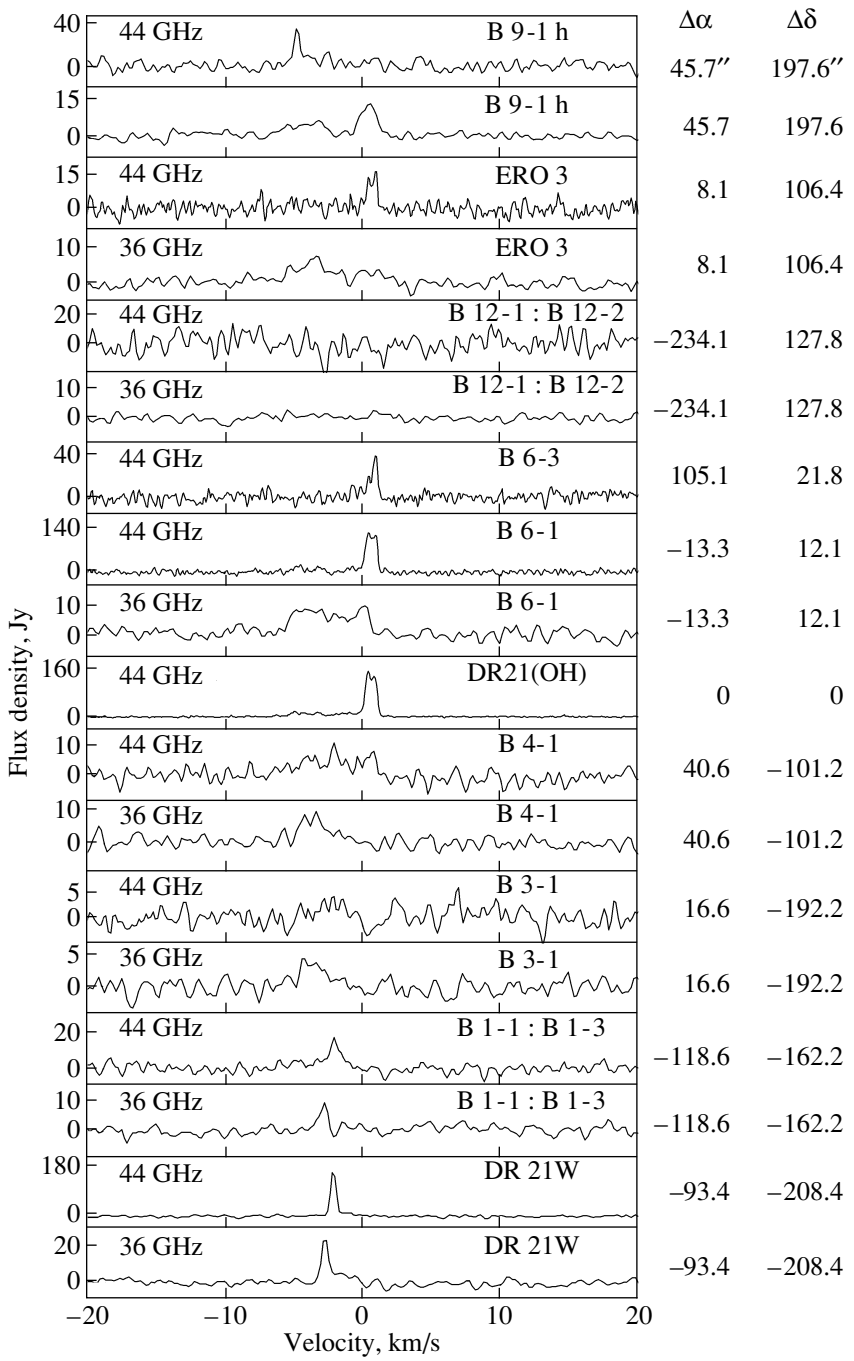

Fig. 1. Observations on the 20-m radio telescope of the Onsala Observatory in 2007. Spectra at 44 and 36 GHz at the positions for our search for methanol emission in knots of molecular hydrogen emission in the $v = 1\text{-}0$ S(1) line. The notation corresponds to that of Davis et al. [13]. The spectra are also given, only at 44 GHz for DR 21(OH) and at both frequencies for DR 21West. Offsets for the studied positions with respect to the pointing center are given at the right.

detected by Mangum et al. [16] in NH_3 and the class II methanol maser DR 21(OH)N detected at 6.7 GHz toward ERO 3 [22]. It is located 106″ to the North of DR 21(OH)main; Pratap et al. [21] suggest a probable association with a molecular condensation detected by Wilson and Mauersberger [27] in the $C^{18}O$ and $C^{34}S$ lines.

Since we are more interested in the association of class I methanol emission with emission of excited hydrogen, we will analyze in detail the situation with regard to the H_2 filaments considered by Davis et al. [13]. Figure 1 presents spectra of the observed lines toward selected directions in order of decreasing declination. The spectra of DR 21(OH) observed by

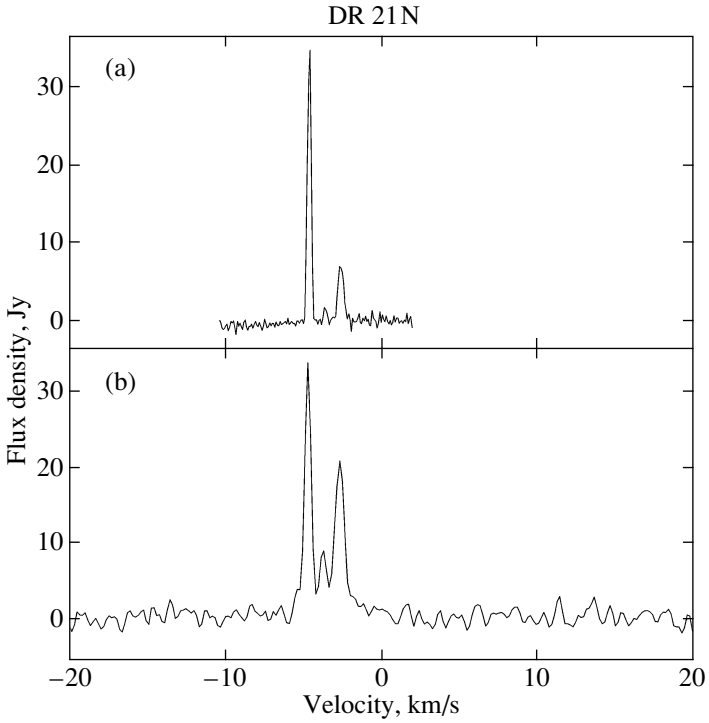

Fig. 2. The new source DR 21N at 44 GHz: (a) spectrum obtained in 2008 on the 20-m Onsala radio telescope, (b) VLA cross-correlation spectrum of 2007 (NRAO archive) obtained on two antennas with a short baseline at the center of the array.

us at 44 GHz and of DR 21West observed at both frequencies are also shown. The names of the spectra are given using the notation of [13] for the corresponding pointing positions. We plotted and combined the spectra using the Super Mongo graphics package and corrected the graphics using the Adobe Illustrator software.

Figure 5 shows the map of the 44-GHz class I methanol maser emission in the vicinity of DR 21(OH) obtained in 2008 on the 20-m radio telescope of the Onsala Observatory (the asterisks show the positions for our 2007 search toward regions of molecular hydrogen emission). The contours correspond to levels from approximately 10 to 300 Jy with a step of about 18 Jy. The northern source DR 21N (circle) is new: as noted above, it was first observed in methanol maser lines on the 37-m Haystack antenna [21], then somewhat later by us (the current study).

Figure 6 presents a series of maps of the 44-GHz methanol maser emission in the vicinity of DR 21(OH). The contours are the same as in Fig. 5. The telescope beam is shown in the lower left corner, and velocity intervals are given in the upper right corners of the maps. The velocity resolution is 0.17 km/s.

Below, we give comments for each position we have studied in methanol emission in the structure formed by the H_2 knots and ERO 3, from North to South.

1. Component "h" and the chain of bright H_2 knots B 9-1 (see [13] and references therein) could be either a part of an outflow extending from West to East from a young stellar object at the eastern end of the chain B 9-1 or a fragment of a shock from the South, e.g., from IRS 7, IRS 8, or ERO 3. In 2007, we detected narrow features at velocities from -5 to -3 km/s toward component "h" and a broad thermal feature at 44 GHz, and a blend of two features at 0 km/s at 36 GHz, which is absent at 44 GHz. However, the maximum of the emission from this region is due to DR 21N (as was found by both Pratap et al. [21] and ourselves).

Figure 2 presents two 44-GHz spectra for this source: the Onsala spectrum of 2008 (this work) and a 2007 spectrum from the VLA archive (NRAO). The VLA observations were conducted in the A configuration including all 27 antennas; the cross-correlation spectrum between two close antennas at the center of the array is shown. The adopted rest frequency for the $7_0-6_1A^+$ methanol transition on the VLA was 44069.4 GHz. The source velocity was set at -5 km/s. The pointing position was RA $= 20^h38^m59.280^s$, DEC $= 42°22'48''.70$ (J2000). The source was observed for approximately 2 h 17 min, with a net integration time of 27 min 40 s. The receiver bandwidth Q was 40–50 GHz. In this configuration, the maximum angular resolution is about $0.05''$.

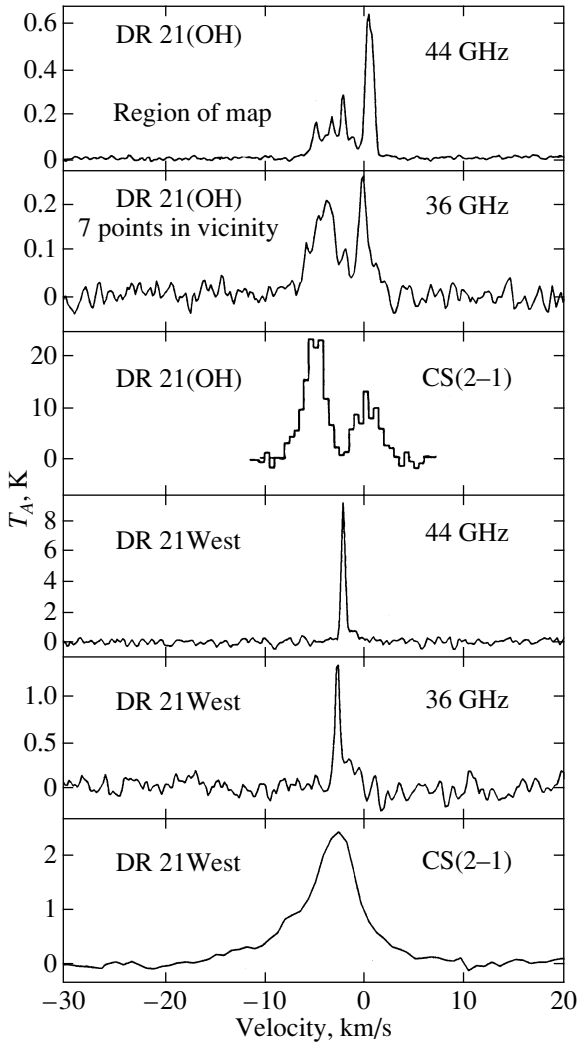

Fig. 3. Averaged 44- and 36-GHz spectra shown in Fig. 1 except for DR 21West, whose spectrum is given in the second and third bottom graphs. Bottom: CS (2–1) spectrum at the position of DR 21West [30]. See text for further information.

The secondary calibrator was the quasar 2007 + 404 (flux density 1.11 Jy at 44 GHz). The observations were conducted in right-circular polarization. An autocorrelator mode with 256 channels and a total bandwidth of 3125 kHz was used, providing spectral resolution of 12.2 kHz at 44 GHz. We processed the data using the AIPS NRAO software package. The VLA spectrum was reduced to the frequency of the Onsala observations. The 44-GHz line parameters for the Onsala spectrum are listed in Table 1.

2. ERO 3 is a bright infrared source at 8 μm [25]. It is a very young massive protostar with an interstellar disk detected in 6.7-GHz class II methanol emission [22, 23]. It is not associated with the H_2 jets [13]; however, 44-GHz methanol maser emission is present at 0 km/s (two features), and 36-GHz emission in the interval from −5 to −3 km/s and, less definitely, near 0 km/s. It is possible that ERO 3 is an independent object at 44 GHz, in the sense that its emission cannot be due to the presence in the telescope beam of emission of the two bright features from DR 21(OH) or the three features from DR 21N. The 44-GHz emission toward ERO 3 is fairly bright; the velocities do not coincide with those for the spectrum of DR 21N, but do coincide with those for DR 21(OH), though ERO 3 is 106″ to the North of DR 21(OH).

3. Farther to the West, there is a group of faint spots and diffuse jets together with the object IRS 10, which may be a collimated outflow associated with an H_2 spot and the faint jet B 12-1 : B 12-2 [13]. We pointed toward the brighter spots B 12-1 : B 12-2; in this case, the entire group was within the beam. No 44

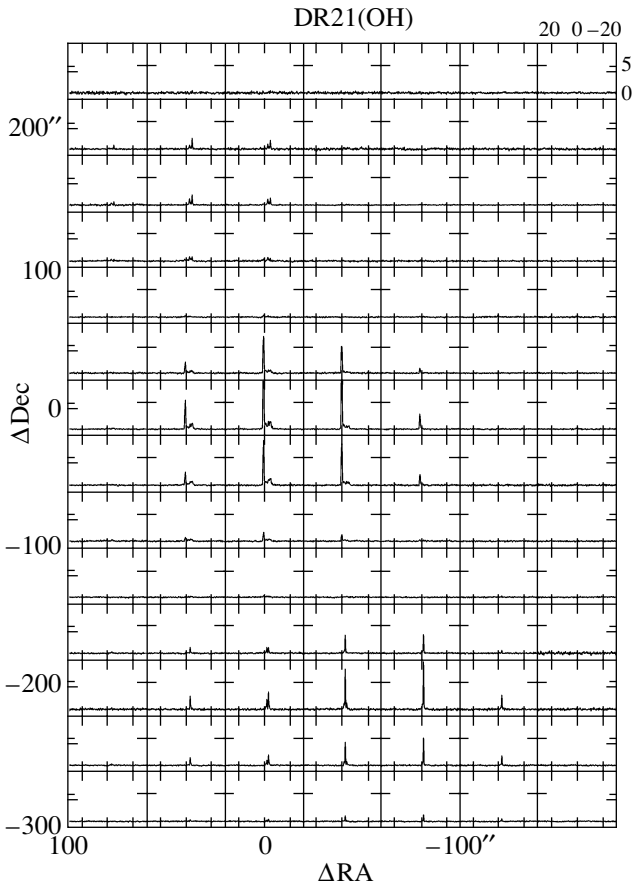

Fig. 4. Position grid of the observations in the $7_0-6_1A^+$ 44-GHz methanol maser line in the vicinity of DR 21(OH) obtained with a spacing of 40″. The map center position is RA(J2000) = $20^h38^m01.01^s$, Dec(J2000) = 42°22′50″.2.

or 36-GHz methanol emission was detected, within upper limits of 6 and 3 Jy, respectively.

4, 5. At the center of the region are DR 21(OH) and the jets labeled B 6-1 : B 6-3 [13]. Together with the jet B 6-1, DR 21(OH) is within the telescope beam. At 44 GHz, the shape of the jet spectra mirrors the spectrum of DR 21(OH), but the emission weakens from DR 21(OH) toward the jet B 6-1 and further to the jet B 6-3, which is 10″ to the North and 90″ to the West from B 6-1. At 36 GHz, the spectrum of B 6-1 has a feature at 0 km/s and a blend of four narrow features in the interval from −5 to −2 km/s. We did not observe DR 21(OH) and B 6-3 at 36 GHz, and these sources are not shown on the map of Fig. 5.

6. Davis et al. [13] identified at least two weak compact sources in H_2 emission to the South of the central region: B 3-1 and B 3-2 and the bright knot B 4-1. This group may be related to the object IRS 4. The 44-GHz emission is weak; the 36 GHz emission is slightly stronger at velocities from −5 to 0 km/s.

7. Another group of H_2 spots toward which we pointed is the knotty arc B 1-1 : B 1-3. The spectra in this region are identical to those of DR 21West at both frequencies, but their emission is weaker.

Thus, observations toward H_2 emission knots have revealed the presence of maser emission at velocities from approximately −5 to −3 km/s, not at 0 km/s, where the strongest maser emission is observed in the central source. In the central source, emission is also present at velocities from −5 to −3 km/s, but is much weaker than the main features and is spatially in another location [12, 17–19].

Figure 3 presents total averaged spectra at 44 and 36 GHz. The top graph shows the spectrum for the vicinity of DR 21(OH) generated from the map obtained in our observations with a spectral resolution of 0.17 km/s. The second graph shows the 36-GHz spectrum for the vicinity of DR 21(OH) obtained from all pointings for our first set of observations (Fig. 1), including DR 21West. The third graph shows the spectrum of the thermal CS (2–1) line, which traces quiescent, dense gas in the molecular cloud (the spectrum is generated from a map obtained at a position between the eastern and western groups

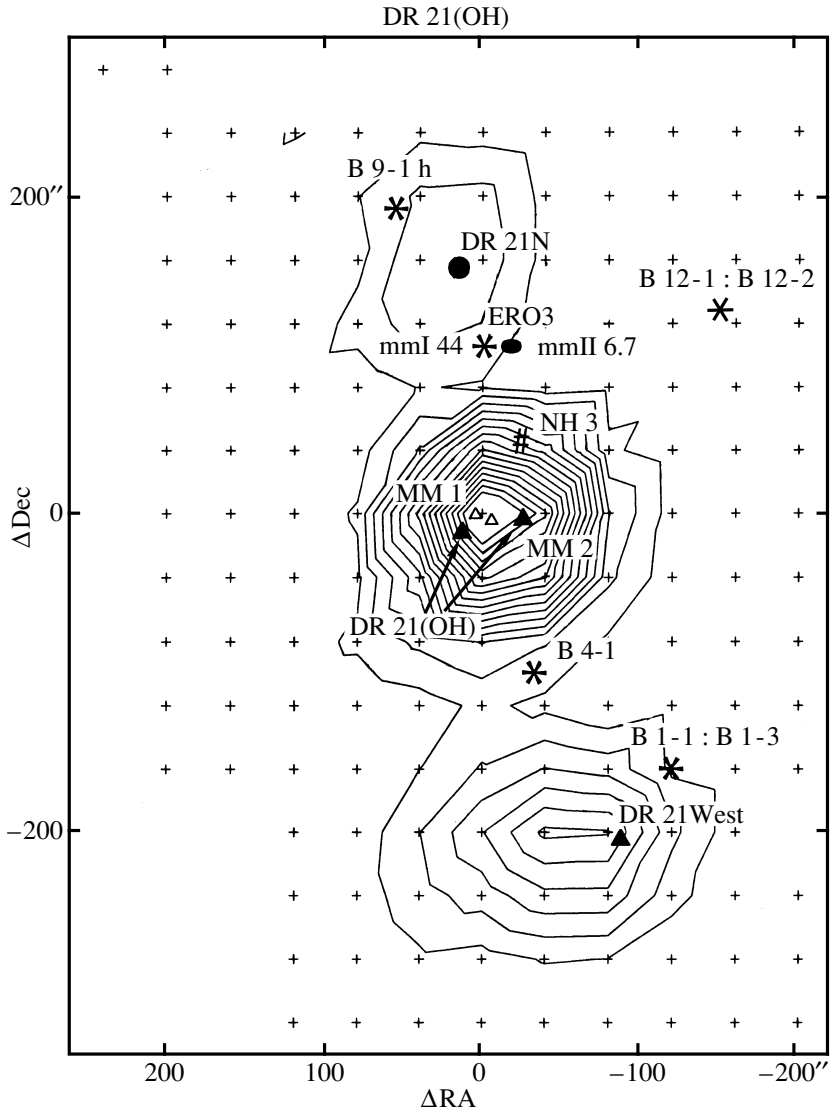

Fig. 5. Map of class I methanol maser emission at 44 GHz in the vicinity of DR 21(OH) (the asterisks show the pointings for the 2007 search toward positions of molecular hydrogen emission) obtained in 2008 on the 20-m radio telescope of the Onsala Observatory. Contours correspond to levels from approximately 10 to 300 Jy with a step of 18 Jy. The central source—DR 21(OH)—is shown by filled triangles. The southern source B 1-1 : B 1-3 gravitates toward the powerful bipolar outflow DR 21. The northern source DR 21N (circle) is new. Millimeter continuum sources (MM1 and MM2, open triangles), a dense NH_3 clump (hash sign), and recently discovered disk (dark horizontal oval) emitting class II 6.7-GHz methanol emission [30] at the position of the infrared source ERO 3 [13] are shown. The source DR 21West is also shown with a filled triangle.

of maser spots in DR 21(OH) with a spectral resolution of 0.5 km/s, taken from [11]). The fourth and fifth graphs present the spectra of DR 21West at the two frequencies in our observations. The sixth graph shows a CS (2–1) spectrum toward DR 21West taken with a resolution of 0.7 km/s [30].

We conclude from an analysis of these spectra that the weaker 44-GHz maser emission "wanders" in the velocity interval from −5 to −2 km/s (for comparison, the velocities of the main features are −4.6 km/s in DR 21N, 0.4 km/s in DR 21(OH), and −2.1 km/s in DR 21West); it is observed at the same velocities as the 36-GHz quasi-thermal emission. 36 GHz emission is definitely present toward B 9-1 h, ERO 3, B 6-1, B 4-1, B 3-1, and B 1-1 : B 1-3. The same velocity range for the 44-GHz maser features is listed in [18].

With regard to the fact that the source of the bipolar outflow of the material in DR 21(OH) remains unknown [17, 18] and the intensity of the eastern wing of the components of DR 21(OH) is fairly weak but comparable to the intensity of the observed spectral

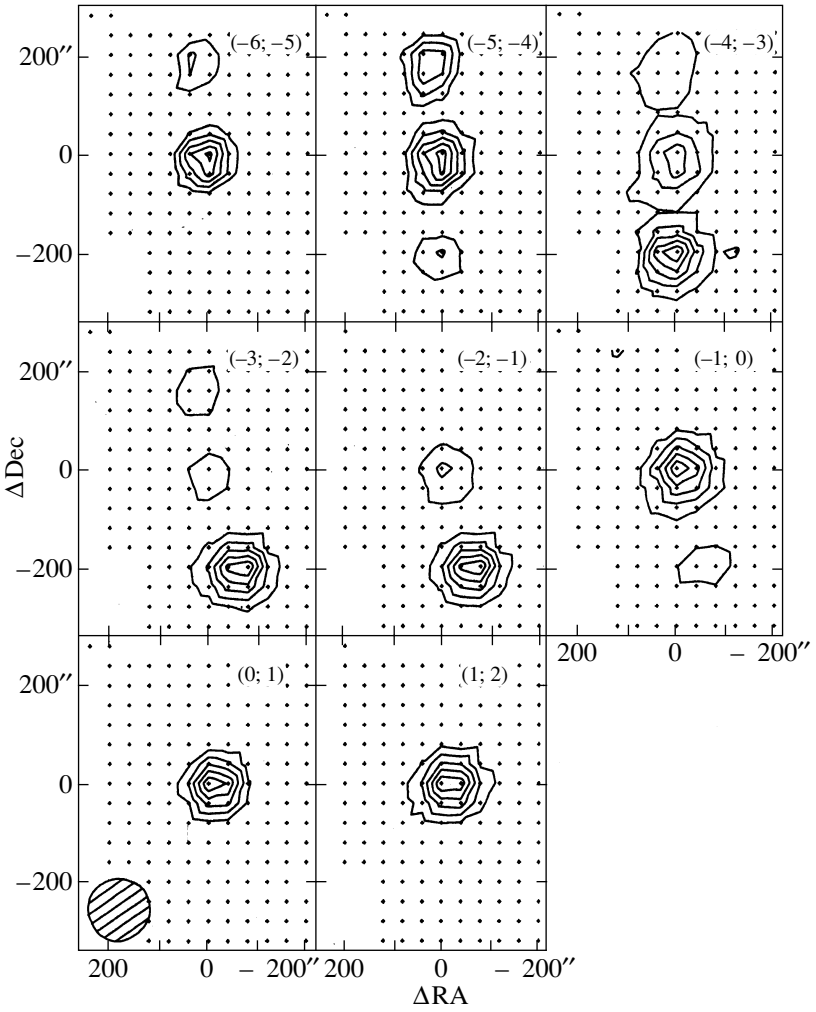

Fig. 6. Series of maps of the 44-GHz methanol maser emission in the vicinity of DR 21(OH) with a velocity resolution of 0.09 km/s. The contours are the same as in Fig. 5. The telescope beam is shown in the lower left corner, and velocity intervals in the upper right corners of the maps. The velocity resolution is 0.17 km/s.

features in the vicinity of the main source on a scale of >400″, we suggest that the fainter eastern components of the DR 21(OH) maser emission are part of an extended region of emission at velocities from −5 to −2 km/s (including the 6.7-GHz class II maser at the center of DR 21(OH), which also has a velocity of −3 km/s [22, 23]), not a component of the bipolar outflow, despite the plausible distribution of spatial components (in the bipolar-outflow hypothesis) [12, 17–19]. Note that the components of the 6.7-GHz class II maser toward ERO 3 have velocities from +3 to +5 km/s [22, 23].

At the same time, the brightening of one of the two brightest maser features noted in [19, 31] implies a zone of activity at a velocity of about 0 km/s, which is probably much smaller in size than the eastern and western components of the DR 21(OH) maser.

The central part of our map covers the region studied by Mangum et al. [7, 16], and this region, including all sources detected in other studies cited above, emits $7_0–6_1A^+$ methanol maser emission on scales of the order of 10 pc (7.5 pc for a distance of 3 or 5 pc for a distance of 2 pc). The observed structure is elongated from North to South, with three pronounced peaks: DR 21N at the top of the map, DR 21(OH) at the center, and near DR 21West in the southern part. Such an extensive region of maser emission could be plausibly produced by numerous fading remnants of shocks, many of which are observed in the vicinity of DR 21(OH) [13]. These remnants could have sufficient energy to excite the rotational–vibrational structure of the molecule, with its subsequent decay and re-radiation of this energy in the maser lines. At the same time, the shocks are not

powerful enough to destroy the methanol molecules. To study fine structure at 44 GHz associated with the spots and jets that emit in molecular hydrogen will require improved spatial resolution and interferometric observations.

4. CONCLUSION

Based on the spatial distribution of the class I methanol maser components in DR 21(OH), we suggested in [19] that such masers might be detected at the positions of H_2 filaments that trace the outflowing gas.

We have accordingly observed gas–dust filaments in the vicinity of DR 21(OH) that emit weakly in the 1-0 S(1) molecular-hydrogen line at the class I methanol maser frequencies of 36 and 44 GHz. We have detected maser methanol emission at 44 GHz, together with maser and quasi-thermal emission at 36 GHz.

To investigate the possible coincidence of the detected sources with H_2 filaments, we mapped the vicinity of DR 21(OH) at 44 GHz.

We have observed with the Onsala radio telescope an extended region of faint maser emission at 44 GHz with three peaks, two of them located toward the central part DR 21(OH) and southern part (DR 21West) of the region. The third peak, DR 21N, is new [21], and our observations confirm its existence.

The observed extended region is elongated North–South, and its linear size is approximately a factor of ten larger than the size of the main emission region at 44 GHz in DR 21(OH). All other structures are embedded in it, including the ERO 3 protostellar disk detected earlier at 6.7 GHz [22, 23].

The spatial resolution of our map does not allow us to distinguish structures at 44 GHz that are associated with spots and jets emitting in molecular hydrogen: the entire region must be studied with higher spectral and spatial resolution and with higher sensitivity.

We suggest that all class I methanol masers are embedded in similar extended structures, making such studies promising. The same considerations were presented in [32]. In particular, it was noted that data on low-brightness extended maser emission can provide clues about the physical conditions in regions of formation of massive stars.

It would likely be fruitful to study the region to the south of DR 21West in detail as well.

ACKNOWLEDGMENTS

This work was partially supported by the Russian Foundation for Basic Research (project nos. 07-02-00248 and 10-02-00147a), the Basic Research Program of the Division of Physical Sciences of the Russian Academy of Sciences on "Active Processes and Stochastic Structures in the Universe," the Program of State Support for Leading Scientific Schools of the Russian Federation (grant no. NSh-626.2008.2), and the Science and Education Center of the Federal Targeted Program in Science and Technology (grant no. 2009-1.1-126-056-018). We are grateful to the staff of the Onsala Observatory for the opportunity to observe on the telescope and for their help with the observations, personally to Lars E.B. Johansson, Roger Hammargren, and especially to Per Bergman, in particular, for the convenient data processing software XS. We also thank the NRAO for granting open access to the archival VLA data for DR 21N. We are grateful to V.I. Slysh for help with the formulation of the problem, attention, and concern for our work, and also to S.V. Kalenskiĭ for help with the observations and correction of the manuscript.

REFERENCES

1. S. V. Kalenskii, Astron. Zh. **72**, 524 (1995) [Astron. Rep. **39**, 465 (1995)].
2. R. M. Lees, Astrophys. J. **184**, 763 (1973).
3. D. M. Cragg, K. P. Johns, and P. D. Godfrey, et al., Mon. Not. R. Astron. Soc. **259**, 203 (1992).
4. R. Bachiller, S. Liechti, C. M. Walmsley, et al., Astron. Astrophys. **295**, L51 (1995).
5. S. Leichti and C. M. Walmsley, Astron. Astrophys. **321**, 625 (1997).
6. I. E. Val'tts and G. M. Larionov, Astron. Zh. **84**, 579 (2007) [Astron. Rep. **51**, 519 (2007)].
7. J. G. Mangum, A. Wooten, and L. G. Mundy, Astrophys. J. **378**, 576 (1991).
8. S.-P. Lai, J. M. Girart, and R. M. Crutcher, Astrophys. J. **598**, 392 (2003).
9. S.-P. Lai, T. Velusamy, and W. D. Langer, Astrophys. J. **596**, L239 (2003).
10. J. P. Vallée and J. D. Fiege, Astrophys. J. **636**, 332 (2006).
11. R. L. Plambeck and K. M. Menten, Astrophys. J. **364**, 555 (1990).
12. L. Kogan and V. Slysh, Astrophys. J. **497**, 800 (1998).
13. C. J. Davis, M. S. N. Kumar, G. Sandell, et al., Mon. Not. R. Astron. Soc. **374**, 29 (2007).
14. M. S. N. Kumar, C. J. Davis, J. M. C. Grave, et al., Mon. Not. R. Astron. Soc. **374**, 54 (2007).
15. M. S. N. Kumar, R. Bachiller, C. J. Davis, et al., Astrophys. J. **576**, 313 (2002).
16. J. G. Mangum, A. Wooten, and L. G. Mundy, Astrophys. J. **388**, 467 (1992).
17. S. Kurtz, P. Hofner, and C. V. Álvarez, Astrophys. J. Suppl. Ser. **155**, 149 (2004).

18. E. D. Araya, S. Kurtz, P. Hofner, and H. Linz, Astrophys. J. **698**, 1321 (2009).
19. S. V. Polushkin, I. E. Valtz, and V. I. Slysh, Astron. Zh. **86**, 134 (2009) [Astron. Rep. **53**, 113 (2009)].
20. M. A. Voronkov, K. J. Brooks, A. M. Sobolev, S. P. Ellingsen, et al., Mon. Not. R. Astron. Soc. **373**, 411 (2006).
21. P. Pratap, P. A. Shute, T. S. Keane, et al., Astron. J. **135**, 1718 (2008).
22. L. Harvey-Smith, R. Soria-Ruiz, A. Duarte-Cabrall, and R. J. Cohen, Mon. Not. R. Astron. Soc. **384**, 719 (2008).
23. L. Harvey-Smith and R. Soria-Ruiz, Mon. Not. R. Astron. Soc. **391**, 1273 (2008).
24. B. L. Ulich and R. W. Haas, Astrophys. J. Suppl. Ser. **30**, 247 (1976).
25. A. P. Marston, W. T. Reach, A. Noriega-Crespo, J. Rho, et al., Astrophys. J. Suppl. Ser. **154**, 333 (2004).
26. K. M. Menten, Astrophys. J. **380**, L75 (1991).
27. T. L. Wilson and R. Mauersbeger, Astron. Astrophys. **239**, 305 (1990).
28. D. P. Woody, S. L. Scott, N. Z. Scoville, et al., Astrophys. J. **337**, L41 (1989).
29. K. J. Richardson, G. Sandell, and K. Krisciunas, Astron. Astrophys. **224**, 199 (1989).
30. G. M. Larionov, I. E. Val'tts, A. Winnberg, et al., Astron. Astrophys. Suppl. Ser. **139**, 257 (1999).
31. P. Pratap, S. Hoffman, and V. Strelnitski, Bull. Amer. Astron. Soc. **38**, 948 (2007).
32. M. R. Pestalozzi, in *Proc. IAU Symp. No. 242 on Astrophysical Masers and their Environment*, Ed. by J. Chapman and W. Baan (Cambridge Univ., Cambridge, 2008), p. 89.

Translated by G. Rudnitskii